

Laboratory and Computing Methods

THE APPLICATION OF MONTE CARLO METHOD TO QUANTITATIVE ELECTRON PROBE MICROANALYSIS OF SILICATE GLASS

JANA NEBESÁŘOVÁ, VÁCLAV HULÍNSKÝ*

South Bohemian Biological Centre, Branišovská 31, 370 05 České Budějovice,

**Institute of Chemical Technology, Department of Glass and Ceramics, Technická 5, 166 28 Prague 6*

Received 11. 6. 1991

The aim of this work was to test Monte Carlo method for the quantitative analysis of silicate glass. The binary glass $PbO-SiO_2$ was chosen for expected big atomic number correction and absorption correction due to large atomic number difference of elements contained in it. It was shown that it is sufficient to simulate some hundreds of trajectories of primary electrons for obtaining the stable values of measured intensity. Linear division of trajectory is more convenient for routine quantitative analysis as well as finest division of the trajectory in steps.

INTRODUCTION

The present extension of computers brings the new possibilities in using theoretical correction procedures even in current practice of quantitative microanalysis. Beside the routine corrections so called ZAF procedure which gives the reliable results in case of bulk sample limited by perfectly flat and smooth surface the simulation of electron penetration through the solid and characteristic X-ray excitation by Monte Carlo method is more frequent at present. This method permits to analyse quantitatively such samples where the excited volume includes more areas with different chemical composition as thin layers, inclusions and free particles. The principle of this method consists in simulation of the individual electrons trajectories penetrating through the solid with simultaneous calculation of the characteristic photons arising along their path. Because the electron penetrating and X-ray emission are random processes the estimations of modelled intensities of X-ray acquired must be necessarily treated by the theory of probability and mathematical statistics. Many models were published [1-5] differing in the description of individual physical phenomena occurring during the scattering of primary electrons in solid and characteristic X-ray excitation. Seldom is this method used in analytical practice. Analysis of metal alloys and semiconductors gives some good results only. The authors have not found any example of the application to silicates in literature. The aim of this work was to use Monte Carlo method for the quantitative analysis of silicate glass.

MONTE CARLO MODEL

The simulation of the electron penetration into glass was performed by means of the Monte Carlo model which was written by Dr. Pavlíček from Nuclear Fuel Institute Zbraslav near Prague [6-9]. This model enables to calculate specific intensities of emitted characteristic X-ray photons per one penetrating electron related to unit spatial angle. In the model an influence of atomic number correction and absorption correction is considered. The fluorescence correction due to characteristic and continuous X-rays radiation is neglected at the glasses with respect to its negligible value. The simulation of one electron path begins with the setting initial conditions of penetration into the solid of defined chemical composition of individual areas. The actual electron path is supplied by the step-like spatial curve which consists of preliminary chosen number of steps. At the final point of each step the basic characteristic of electron are calculated: radius vector r_m , travel direction vector u_m and kinetic energy E_m . Simultaneously new position of electron r_{m+1} , new travel direction u_{m+1} and number of ionizations are determined. By this way, step by step, the simulated trajectory of electron is constructed until the energy of electron drops to value E_{min} stated preliminary. E_{min} is for given case the ionization potential of the edge to that belongs on the measured line of characteristic X-ray.

MULTIPLE SCATTERING

The calculation of the change of unit travel direction vector u_m is calculated according to the theory of multiple scattering proposed by Goudsmith and

Saunderson (8). This theory outcomes from the description of individual elastic scattering of electron characterized by Rutherford scattering cross section. In this theory the mean energy loss of electron in given step due to inelastic scattering is calculated by approximation of continual energy loss of electron. The probability density $f_{GS}(\omega)$ and probability distribution function $F_{GS}(\omega)$ of the random scattering angle ω from the original motion of the electron in the direction given by vector u_m is according to the theory given by

$$f_{GS}(\omega) \sin \omega d\omega = \sum_{k=0}^{\infty} (k+1/2) A_k P_k(\cos \omega) \sin \omega d\omega$$

$$F_{GS} = \int_0^{\infty} f_{GS}(\omega) \sin \omega d\omega = \sum_{k=0}^{\infty} (k+1/2) A_k \int_{\cos \omega}^1 P_k(x) dx$$

where $A_k = \exp[-\int_0^{\theta} G_k(s) ds]$ and $P_k(x)$ is Legendre polynomial of the k order. These coefficients are functions of the trajectory of electron and by means of functions

$$G_k(s) = 2\pi \int_0^{\pi} N \sigma(\theta E(s)) [1 - P_k(\cos \theta) \sin \theta d\theta]$$

they depend also on the density ρ , on the number of atoms N and on the individual elastic scattering cross section σ . θ is the scattering angle for the individual elastic collision. The simulation of the scattering angle ω at multiple scattering is in program carried out by the distribution function $F_{GS}(\omega)$ using the method of inverse functions. The second angle α so called azimuth angle determining the new direction of electron path given by the vector u_{m+1} has uniform distribution within the interval $(0, 2\pi)$.

The change of position vector Δr is expressed as the vector having the longitudinal component $\Delta \zeta$ in the original direction of electron path u_m and with two perpendicular components $\Delta \xi$, $\Delta \eta$ on the plan perpendicular to the vector u_m . The calculation of the components $\Delta \xi$, $\Delta \eta$ as functions of scattering angle ω and azimuth angle α is based on the theory of Rosi according to the following relations:

$$\Delta \xi = \frac{1}{2} s_m \left(\sin \omega \cos \alpha + k_x \sqrt{\frac{\langle \omega \rangle^2}{6}} \right)$$

$$\Delta \eta = \frac{1}{2} s_m \left(\sin \omega \cos \alpha + k_y \sqrt{\frac{\langle \omega \rangle^2}{6}} \right)$$

where s_m is the step length, k_x and k_y are two independent random numbers having normal distribution.

For the calculation $\langle \omega \rangle^2$ the relation given by Berger is used:

$$\langle \omega \rangle^2 = 2(1 - \langle \cos \omega \rangle)$$

where $\cos \omega$ is equal to coefficient A_I in the expressions for probability density $f_{GS}(\omega)$ or probability distribution function $F_{GS}(\omega)$. The longitudinal component is calculated according to Berger's relation

$$\Delta \zeta = \frac{1}{2} s_m (1 + \cos \omega)$$

ELECTRON PATH AND ENERGY LOSS

Electron path in the solid and its energy loss are approximated in MC model by means of Bethe's formula continuous energy loss (6). Our model offers two possibilities of dividing the electron trajectory in steps according to its energy:

a) linear which is given by:

$$h_E = (E_0 - E_{\min}) / M$$

where M is the step number, E_0 is initial energy of electron, E_{\min} is the lowest excitation energy for given series of characteristic lines of analysed elements.

b) logarithmic, where the ratio of energies at the beginning and the end of each step is constant:

$$q_E = E_{k+1} / E_k = \text{const. } k = 0, 1, 2, \dots, M$$

Owing to the use of continuous energy loss approximation the electron path absolved in the solid is related to the loss of its kinetic energy according to:

$$\Delta s_{k,k+1} = s(E_k) - s(E_{k+1}) \quad k = 0, 1, 2, \dots, M$$

The sum of all steps is equal to the total electron path length in solid. Values $s(E_k, E_{k+1})$ are determined with the help of so called standard electron path, that is calculated for given sample from Bethe's law for stopping power within the energy interval 0–50 keV by the parabolic interpolation from three points made in each step of 2 kV. In case the electron path crosses the boundary between two layers with different chemical composition or boundary with the primary path step is divided in further steps linearly according to energy.

CHARACTERISTIC X-RAYS INTENSITY CALCULATION

Bethe's expression for stopping power for ionization cross section were used. First the standard ionization function, defined as the mean number of ionizations induced by electron in given sample on the trajectory corresponding to the drop of its energy from 50 keV to zero level is calculated. This values are determined for each element analysed in individual layers in points corresponding to energy drop of 2 keV. The set of these 26 values is used for the determination of

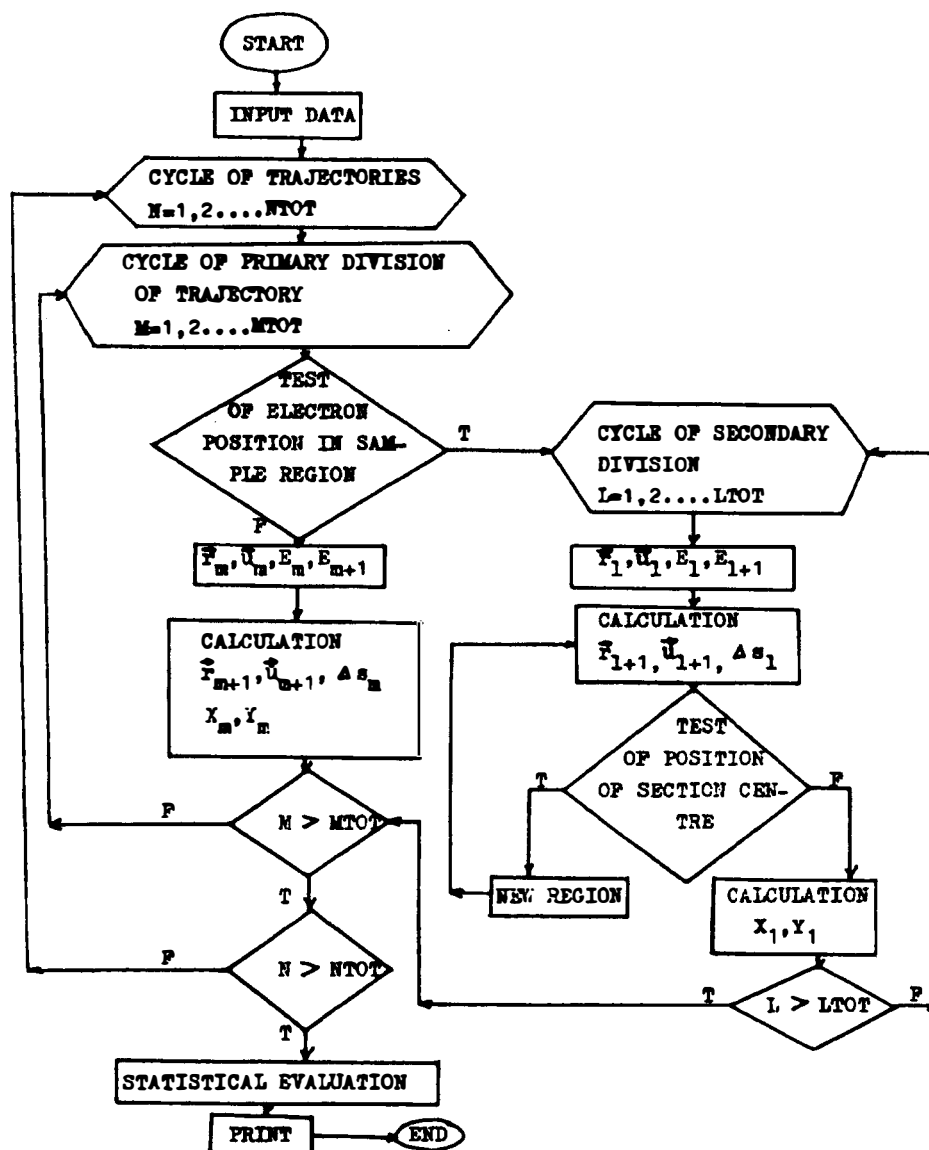


Fig. 1. Flow diagram for the simulation of $NTOT$ electron trajectories in the sample consisted of more areas of different chemical composition with given geometry.

number of ionizations in given step of simulated electron path by parabolic interpolation. Absorption of emitted characteristic X-ray radiation in the sample before its outcome from the surface is calculated in routine way using the exponential absorption factors where distances travelled by emerging X-ray in particular areas are considered. Simulation process of one trajectory is then repeated for more electrons. The contributions of individual trajectories are added to accumulators of simulated quantities and after completing the evaluation takes place. Like output serves the mean value of intensity of X-ray related to one electron and unit spatial angle then the estimation of dispersion variance and of standard deviation of sim-

ulated intensity takes place. Because the basic value in quantitative EMA is the relative intensity which is equal to the ratio of intensities measured at the same conditions on sample and standard no absolute value of X-ray intensity is not necessary to calculate. So the author avoid the use of some not quite safely determined atomic constants.

The described MC model became the basis of the computing programme TV(F) by means of which we provided the calculations. The simplified flow diagram of the whole programme is drawn in Fig. 1.

Table I

The composition of lead glass

c[wt. %]	Pb	Si	O
Pb-9	50.697	20.996	27.897
Pb-6/2	66.111	13.431	20.458

Table II

Constants used for simulation of electron microanalysis of lead glass [10, 11]

Element	Z	EX [keV]	Analyzed line	λ [Å]
Si	14	1.840	K(α_1)	7.125
Pb	82	2.484	M(α_1)	5.286

 μ [cm²g⁻¹]

Emitter \ Absorber	Si	Pb	O
Si	327.9	1908.6	965.6
Pb	1862.1	983.0	415.7

EXPERIMENTAL

The binary glass PbO-SiO₂ was chosen for application the programme TV(F). The composition of analyzed glasses which were prepared as reference standards and served for many years in our laboratory for measurement of lead glass is introduced in Table I. This simple three-element system was chosen tendentiously. The reason is the homogeneity of glass, exactly defined and justified composition and mainly expected distinct atomic number correction and absorption correction due to big atomic number difference of element contained in this glass. First approach to the TV(F) programme is characterized by our effort to find answers on following questions: 1) How many electron trajectories to simulate, thus how quickly converged the simulated primary generated intensity and measured intensity of characteristic X-ray to some limit value? 2) How to divide the trajectory and in how many steps divide it? 3) How to procedure of dividing mentioned above affects the results of simulating? The calculations were provided by computer ICL-4-72 for accelerating voltage

Table III

Primary generated intensity XM and detected intensity YM of SiK α line and PbM α line for various number of simulated trajectories in glass Pb-6/2, U = 20 keV, sXM, sYM - standard deviations of primary and detected intensity

a) silicon

NTOT	XM	sXM	YM	sYM
100	2.66E-3	1.1E-4	1.61E-3	6.4E-5
200	2.65E-3	7.5E-4	1.59E-3	4.5E-5
300	2.63E-3	6.2E-4	1.54E-3	3.7E-5
400	2.61E-3	5.4E-4	1.54E-3	3.2E-5

b) lead

NTOT	XM	sXM	YM	sYM
100	3.21E-3	1.2E-4	2.36E-3	8.6E-5
200	3.19E-3	8.6E-5	2.33E-3	6.0E-5
300	3.16E-3	7.2E-5	2.28E-3	4.9E-5
400	3.15E-3	6.3E-5	2.27E-3	4.3E-5

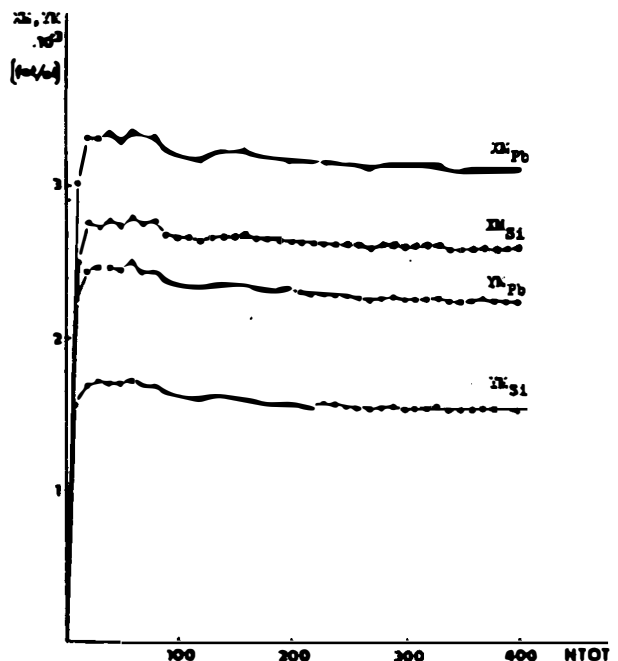


Fig. 2. Convergence rate of primary generated intensity XM and detected intensity YM of X-ray K α line of Si and M α line of Pb at the simulation of X-ray emission from glass Pb-6/2 by MC method.

Table IV

Primary generated intensity XM and detected intensity YM of SiK_α line and PbM_α line determined for different steps number M of linear and logarithmic division of individual trajectory during the simulation of primary electron penetration in glass Pb-9, standard Pb-6/2, $U = 20$ kV

A) linear division: silicon

NDPT	NTOT	h_E	$XM/10^{-3}$	$sXM/10^{-4}$	$YM/10^{-3}$	$sYM/10^{-5}$	XM/YM
5	100	3.63	4.05	1.1	2.38	8.0	0.59
10	100	1.82	3.71	1.4	2.42	9.0	0.65
15	100	1.21	3.60	1.5	2.23	8.9	0.62
20	70	0.91	3.78	1.6	2.42	1.0	0.64
25	70	0.73	3.54	1.8	2.21	1.0	0.62
30	50	0.61	3.51	2.2	2.22	1.03	0.63

lead

NDPT	NTOT	h_E	$XM/10^{-3}$	$sXM/10^{-4}$	$YM/10^{-3}$	$sYM/10^{-5}$	XM/YM
5	100	3.50	2.39	0.6	1.64	4.6	0.69
10	100	1.75	2.19	0.8	1.62	5.6	0.74
15	100	1.17	2.13	0.9	1.52	5.7	0.71
20	70	0.88	2.24	0.9	1.63	6.3	0.73
25	70	0.70	2.10	1.0	1.51	6.8	0.72
30	50	0.58	2.08	1.2	1.51	8.5	0.72

B) logarithmic division: silicon

NDPT	NTOT	q_E	$XM/10^{-3}$	$sXM/10^{-4}$	$YM/10^{-3}$	$sYM/10^{-5}$	XM/YM
8	100	0.74	4.08	1.0	2.35	7.7	0.58
10	100	0.79	3.79	1.3	2.26	7.5	0.60
12	100	0.82	3.97	1.2	2.37	7.9	0.60
14	100	0.84	3.77	1.3	2.33	8.1	0.62
16	100	0.86	3.88	1.3	2.30	8.3	0.59
18	50	0.88	3.64	2.1	2.36	13.3	0.65
20	90	0.89	3.87	1.4	2.35	8.5	0.61

lead

NDPT	NTOT	q_E	$XM/10^{-3}$	$sXM/10^{-4}$	$YM/10^{-3}$	$sYM/10^{-5}$	XM/YM
8	100	0.77	2.41	0.55	1.63	0.42	0.68
10	100	0.81	2.24	0.71	1.56	0.45	0.69
12	100	0.84	2.34	0.66	1.62	0.46	0.69
14	100	0.86	2.23	0.74	1.59	0.50	0.71
16	100	0.88	2.29	0.72	1.58	0.50	0.69
18	50	0.89	2.15	1.2	1.58	0.84	0.74
20	90	0.90	2.28	0.79	1.60	0.53	0.70

Table V

Relatives intensities K , absorption correction factors F_a and atomic number correction factor F_z determined for different steps number M of linear and logarithmic division of individual trajectory during the simulation of primary electron penetration in glass Pb-9, standard Pb-6/2, $U = 20$ kV

a) linear division

		Si				Pb			
M	NTOT	K	sK	F_a	F_z	K	sK	F_a	F_z
5	100	1.552	0.005	1.00	0.99	0.722	0.002	0.95	0.99
10	100	1.573	0.006	1.11	0.91	0.715	0.003	1.03	0.91
15	100	1.449	0.006	1.05	0.88	0.669	0.003	0.99	0.88
20	70	1.574	0.008	1.09	0.93	0.720	0.003	1.01	0.93
25	70	1.439	0.008	1.06	0.87	0.664	0.004	1.00	0.87
30	50	1.448	0.012	1.08	0.86	0.666	0.005	1.01	0.86

b) logarithmic division

		Si				Pb			
M	NTOT	K	sK	F_a	F_z	K	sK	F_a	F_z
8	100	1.532	0.005	0.98	1.00	0.72	0.002	0.94	1.00
10	100	1.474	0.005	1.02	0.93	0.686	0.002	0.96	0.93
12	100	1.541	0.005	1.01	0.97	0.72	0.002	0.96	0.97
14	100	1.516	0.005	1.05	0.92	0.700	0.002	0.99	0.92
16	100	1.500	0.006	1.01	0.95	0.70	0.002	0.96	0.95
18	50	1.533	0.012	1.10	0.89	0.70	0.005	1.02	0.89
20	90	1.531	0.006	1.03	0.95	0.71	0.003	0.98	0.95

in the interval 10–20 keV. Necessary constants used for simulation of electron microanalysis of lead glass are summarized in Table II.

To the evaluation of the results of simulation we used the values current in the method ZAF which we calculated from the output values according to the next relations:

Relative intensity is the ratio between detected X-ray intensities of given line measured by the same experimental conditions on the sample and the standard:

$$K = Y_{MS} / Y_{MST}$$

Its standard deviation

$$sK = K \sqrt{\frac{(sY_{MS})^2}{NTOT_S Y_{MS}} + \frac{(sY_{MST})^2}{NTOT_{ST} Y_{MST}}}$$

where Y_{MS} , Y_{MST} , are the mean values of detected X-ray intensities for sample and standard. sY_{MST} , sY_{MS} are its standard deviations.

The absorption correction factor

$$F_a = \frac{X_{MST} Y_{MS}}{X_{MS} Y_{MST}}$$

The atomic number correction factor

$$F_z = \frac{c_{ST} X_{MS}}{c_S X_{MST}}$$

RESULTS AND DISCUSSION

The rate of convergence of primary and detected X-ray radiation of SiK_α line and PbM_α line during the simulation of 20 keV electron penetration in glass Pb-6/2 is introduced in Fig. 2. It is evident that summary number 400 of simulated trajectories is sufficient for setting the mean value of primary and detected X-ray characteristic lines of both analysed elements. The difference between detected intensities for 300 trajectories and 400 trajectories is 0.36% at Si and 0.49% at Pb at the same time. The significant improvement of the statistical estimation take place as follows from

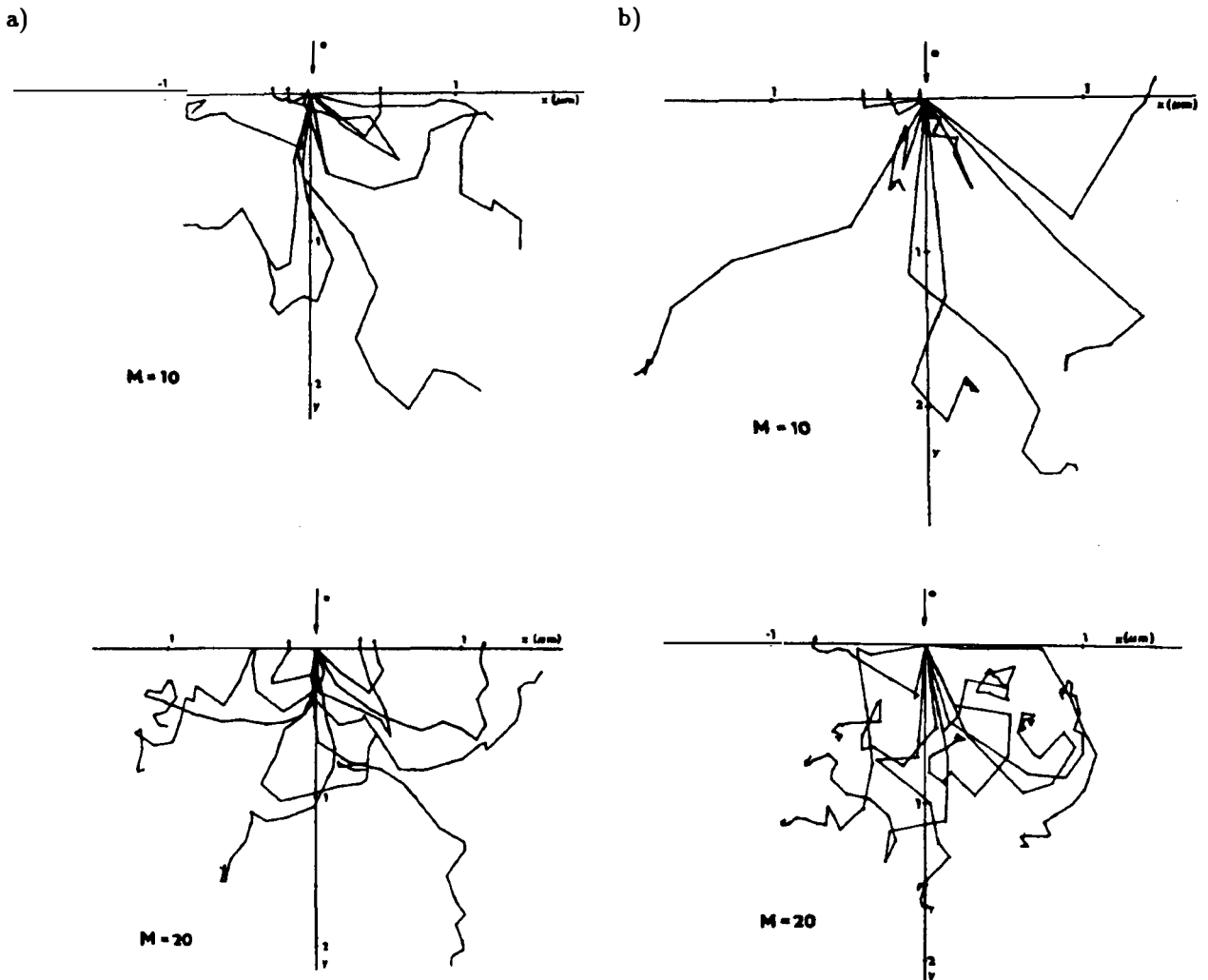


Fig. 3. Ten electron trajectories in glass Pb-9 projected into xz plane, $U = 20$ kV, a) linear division, 10 and 20 steps, b) logarithmic division, 10 and 20 steps.

the standard deviations of primary and detected intensity introduced in Table III. The form of curves in Fig. 2 is approximately identical. The jumps on the curves are due to electron that escapes from the sample before its energy drops under certain value E_{min} . Such a given trajectory then produces less ionizations which causes the drop of mean value of both intensities for both elements.

For estimation of the influence of trajectory division on the simulation results the number of calculations for glass Pb-9 were carried out. These results are presented in Table IV and V. In Table IV there are the output values from the program TV(F) for different steps number of linear and logarithmic division of individual trajectory during the simulation of primary electron penetration in glass Pb-9. We used glass Pb-6/2 as the standard, in the concrete the values of primary generated and detected X-ray intensity for number of simulated trajectories NTOT-400. From

Table V there is apparent some dispersion of relative intensities between analysed elements and between methods of the trajectory dividing. The cause is like the random character of emission of X-ray like the different number of simulated trajectories of glass Pb-9. As significant we consider the difference in atomic number factors that are higher for logarithmic division of trajectory. The influence of nonuniform length of individual steps plays role here. The first step is always longest and electron after passing is penetrates rather deep into the sample decreasing the probability of backscattering. Various shapes of trajectories at linear and logarithmic division are documented in Fig. 3.

Logarithmic division of trajectory according to electron energy seems to be more suitable for simulation the electron penetration accelerated by higher voltage. When using it for simulation of the electron penetration through the thin layer it is necessary to

Table VI

Mean lengths of first steps simulated electron trajectories

a) linear division, various number of steps,
U = 20 kV

M	5	10	15	20	25	30
s(μm)	2.15	1.17	0.8	0.61	0.50	0.41

b) logarithmic division, various number of steps,
U = 20 kV

M	8	10	12	14	16	18	20
s(μm)	2.57	2.24	1.99	1.79	1.61	1.47	1.35

c) various accelerating voltage, linear
division, M = 20

U(kV)	10	15	20	25	30
s(μm)	0.16	0.36	0.61	0.92	1.29

compare the thickness of such layer with the length of the first step to avoid electrons passing through this layer. In Table VI all calculated length of first steps for linear and logarithmic division for various accelerating voltages and various numbers of steps are presented.

CONCLUSION

Presented MC model based on the theory of multiple scattering and approximation of continuous energy loss of energy was used to simulation of electron penetration to lead glass. It was shown that it is sufficient to simulate hundreds of trajectories for obtaining the stable values of primary and detected X-ray intensity. For the routine quantitative analysis (20 kV) it is more convenient to use the linear division of the trajectory and as high number of steps as possible. To nonuniformity of the steps lengths at logarithmic division negatively increases the value of atomic number correction factor.

Used symbols:

\mathbf{r} radius vector of electron
 \mathbf{u} travel direction vector of electron
 E electron energy
 F_0 initial electron energy
 E_{\min} minimal electron energy equals to ionization potential of given X-ray spectral series
 $f_{GS}(\omega)$ probability density of the random scattering angle of electron
 $F_{GS}(\omega)$ probability distribution function of the

scattering angle of electron
 N number of atoms
 σ individual elastic scattering cross section
 θ scattering angle for individual elastic collision
 ω scattering angle at multiple scattering
 α azimuth angle
 $\Delta\xi\Delta\eta$ perpendicular components of the radius vector of electron
 $\Delta\zeta$ longitudinal components of the radius vector of electron
 s trajectory length
 s_m m -step length
 k_x, k_y independent random numbers
 h, q step at linear and logarithmic distribution
 M step number at primary distribution
 L step number at secondary distribution
 $NTOT$ total number of simulated trajectories
 K relative intensity
 sK standard deviation of relative intensity
 X primary generated X-ray intensity of given line
 XM mean value of primary generated X-ray intensities of given line
 Y detected X-ray intensity of given line
 YM mean value of detected X-ray intensities of given line
 F_a absorption correction factor
 F_z atomic number correction factor
 U accelerating voltage
 Z atomic number
 EX excitation potential
 λ wavelength

μ	mass absorption coefficient
S	sample
ST	standard

References

- [1] Heinrich, K. F. J., Newbury, D. E., Yakowitz, Y. (eds.): *Use of Monte Carlo Calculations in Electron Probe Microanalysis and Scanning Electron Microscopy*, Nat. Bur. Stds. Spec. Publ. 460, Washington 1976.
- [2] Shimizu, R., Nishigori, N., Murata, K.: Proceedings of The Sixth Int. Conference on X-ray optics and microanalysis, eds. G. Shinoda, K. Kohra, T. Ichinokawa, Osaka 1971, p. 95.
- [3] Murata, K., Matsukawa, T., Shimizu, R.: Proceedings of The Sixth Int. Conference on X-ray optics and microanalysis, eds. G. Shinoda, K. Komra, T. Ichinowa, Osaka 1971, p. 105.
- [4] Henoc, J., Maurice, F.: Proceedings of The Sixth Int. Conference on X-ray optics and microanalysis, eds. G. Shinora, K. Kohra T. Ichinokawa, Osaka 1971, p. 113.
- [5] Ho, Y. C., Chen, J. G., Wang, X. L.: *Scanning Microscopy*, Vol. 3, No. 3, 725 (1989).
- [6] Pavlíček, M.: The simulation of quantitative microanalysis by Monte Carlo I. Theoretical base of the method and description of system Moncapac. Research report UJP 459, Prague 1977.
- [7] Pavlíček, M.: The simulation of quantitative microanalysis by Monte Carlo II. The microanalysis of selected binary intermetallic phases. Research report UJP 486, Prague 1979.
- [8] Pavlíček, M.: The simulation of quantitative microanalysis by Monte Carlo III. The application of M. C. to microanalysis of Zr alloys. Research report UJP 519, Prague 1980.
- [9] Pavlíček, M.: The simulation of quantitative microanalysis by M. C. Proc: Seminary on EMA and SEM, Poljanka 1983.
- [10] *Progress in Nuclear Energy, Series IX Analytical Chemistry*, Volume 9, Eds. H. A. Elion, D. C. Stewart, Pergamon Press 1969.
- [11] Heinrich K. F. J.: *The Electron Microprobe*, eds. T. D. McKinley, K. F. J. Heinrich, D. B. Wittry, Wiley New York, 1966.

**POUŽITÍ METODY MONTE CARLO KE
KVANTITATIVNÍ RTG. MIKROANALÝZE SKEL**

JANA NEBESÁŘOVÁ, VÁCLAV HULÍNSKÝ

*Společné laboratoře biologických pracovišť ČSAV,
Jihočeské biologické centrum, Branišovská 31,
370 05 České Budějovice
Vysoká škola chemicko-technologická, Ústav skla
a keramiky, Technická 5, 166 28 Praha 6*

Současný rozvoj počítačové techniky poskytuje nové možnosti v použití náročných korekčních teoretických postupů v běžné praxi kvantitativní rtg. mikroanalýzy. Uvedený model výpočtu korekcí pomocí metody Monte Carlo, použitý k modelování průniku primárních elektronů do olovnatých skel, je založen na teorii mnohonásobného rozptylu a aproximaci spojitých ztrát energie primárních elektronů. V práci bylo prokázáno, že stačí modelovat stovky trajektorií primárních elektronů k dosažení stabilních hodnot primární a detekované intenzity charakteristického rtg. záření. Dále bylo odzkoušeno, že pro rutinní kvantitativní analýzu je vhodnější lineární dělení trajektorie na co nejmenší úseky. Nerovnoměrné rozdělení délky jednotlivých úseků při logaritmickém dělení způsobí, že hodnota koeficientu korekce na atomové číslo se příliš nahnodnocuje.

Obr. 1. Vývojový diagram modelování souboru $N TOT$ trajektorií elektronů ve vzorku složeném z více oblastí odlišného chemického složení.

Obr. 2. Rychlost konvergence primárně generované intenzity XM a vystupující intenzity YM rtg. záření K_{α} čáry Si a M_{α} čáry Pb, při modelování emise rtg. záření ze skla Pb-6/2 metodou MC.

Obr. 3. Deset trajektorií elektronů ve skle Pb-9 znázorněných v průmětu do roviny xz , $U = 20$ kV, a) lineární dělení na 10 a 20 úseků, b) logaritmické dělení na 10 a 20 úseků.